Virpertron: A novel approach for a virtual cathode oscillator design

Alexander E. Dubinov,[1,2] Alexey G. Petrik,[3] Semen A. Kurkin,[3] Nikita S. Frolov,[3] Alexey A. Koronovskii,[3] and Alexander E. Hramov[3,a)]

[1]*National Research Nuclear University "MEPhI," 31 Kashirskoe Highway, Moscow 115409, Russia*
[2]*Sarov State Institute of Physics and Technology (SarFTI) of National Research Nuclear University "MEPhI," 6 Dukhova Str., Sarov, Nizhni Novgorod Region 607186, Russia*
[3]*Saratov State Technical University, 77 Politechnicheskaya str., Saratov 410054, Russia and Saratov State University, 83 Astrakhanskaya str., Saratov 410012, Russia*

(Received 24 October 2016; accepted 6 June 2017; published online 28 June 2017)

In this paper, we propose a novel approach for the design of a virtual cathode oscillator. As a new concept, we suggest a microwave system containing an annular relativistic electron beam travelling through the drift space with dielectric inserts characterized by different values of permittivity. In this case, a virtual cathode which is the source of powerful electromagnetic oscillations forms at the junction of different dielectric materials. According to the mechanism of virtual cathode formation, we have called this device as a *virpertron*. We have carried out a detailed numerical investigation of virtual cathode formation features in this system via 3D electromagnetic PIC-simulation using CST Particle Studio. We have also studied the spectral properties of the microwave radiation generated by the virpertron. *Published by AIP Publishing.*
[http://dx.doi.org/10.1063/1.4989715]

I. INTRODUCTION

Virtual cathode (VC) oscillators are a special class of microwave generators for which a multi-gigawatt level of microwave radiation has been achieved several decades ago.[1–3] This class of microwave generators is represented by vircators, reflex triodes, reditrons, and virtodes. The schemes of VC generators, their operation principles, and main achievements are provided, particularly, in Refs. 4–10.

A typical scheme of VC oscillator has a sequence of two vacuum chambers with a high-current electron beam moving inside. In the first chamber (gun area), the beam is generated and accelerated. In the second chamber (drift chamber), it slows down and forms a VC. Oscillations of the VC as an integral electronic structure are the source of powerful microwave radiation. For a VC to be formed in the second chamber, the electron beam transmission capacity of the second chamber should be lower than the capacity of the first chamber. Thus, it is necessary to ensure that the second region has a lower limiting vacuum (or critical) current than the first region ($I_{lim2} < I_{lim1}$).[10–12] Typically, this is achieved by making the cross-sectional area of the second region larger than the first region (as in vircators, reditrons, and virtodes) or by introducing a decelerating electric field in the second chamber (as in reflex triodes and low-voltage vircators). In this paper, we present a new microwave oscillator in which the $I_{lim2} < I_{lim1}$ condition is achieved using a conceptually different approach.

We know that if a chamber is filled with a dielectric with a permittivity ε, the limiting current in the chamber will increase in proportion to ε compared to the vacuum. From an analytical point of view, this is easily explained by the fact that in the right-hand part of Poisson's equation that is used for deriving limiting current values, the space-charge density in the presence of a dielectric is divided by ε : $\Delta\varphi = 4\pi\rho/\varepsilon$. Thus, the dielectric environment reduces the repulsive force of the space charge by a factor of ε. Therefore, if the first and second chambers have equal cross-sections and are filled with dielectrics with dielectric permittivities of ε_1 and ε_2, respectively, and if the $\varepsilon_1 > \varepsilon_2$ condition is fulfilled, it is possible to create conditions for the VC formation only in the second chamber.

A vircator, in which the formation of VC is ensured by filling the chambers with dielectrics with different permittivity values, will be referred to as a *virpertron* (abbreviation from "*vircator*" + "*permittivity*").

We can clearly predict the advantages of the new scheme of VC formation in the virpertron. First, the oscillator becomes geometrically more compact in its cross-sectional dimensions compared to classical vircators. The dynamics of VC formation in a dielectric environment has been considered earlier in Refs. 13 and 14, and the special aspects of high-current beam formation in a two-layer dielectric have been investigated in Ref. 27. Analysis of these works shows the formulation of the second new important functional advantage of a virpertron. Specifically, it is possible to form a VC in the regime of Cherenkov radiation of electrons when their velocity exceeds the velocity of light in a dielectric medium. When the chambers have a waveguide form, to ensure the Cherenkov radiation regime, the velocity of electrons must exceed the phase velocity of the electromagnetic wave in the waveguide.[10,15]

II. VIRPERTRON DESIGN AND FEATURES

To verify the operability and to investigate the proposed virpertron design, 3D PIC-modelling in the CST Particle Studio 2016 (Ref. 16) package has been performed. Previously,

a)Electronic mail: hramovae@gmail.com

this approach has been successfully used to model VC oscillators.[9,17,18]

Virpertron geometry including the dimensions is shown in Fig. 1. The assumption is that the first chamber is filled with a dielectric with a permittivity of ε_1 and the second chamber is filled with vacuum, characterised by a permittivity of $\varepsilon_2 = 1$. In the first region of the system, in a dielectric, a thin cylindrical channel is created, through which the annular electron beam can propagate. It is assumed that the uniform magnetic field with an induction value of 3 T is applied to the virpertron, which is necessary for the propagation of the annular electron beam through the narrow drift channel. The operational principle of the proposed virpertron is similar to that of magnetically insulated vircators, which has been suggested in Ref. 19 and experimentally studied in Refs. 20–22.

A cylindrical annular monovelocity relativistic electron beam with a constant current of $I = 2.5\,\mathrm{kA}$ and an electron energy of $T = 200\,\mathrm{keV}$ is injected in the channel. The following geometric parameters are used for the virpertron simulation: $L_1 = 60\,\mathrm{mm}$, $L_2 = 20\,\mathrm{mm}$, $R_1 = 5\,\mathrm{mm}$, $R_2 = 9\,\mathrm{mm}$, $R_3 = 15\,\mathrm{mm}$, $R_{1b} = 6\,\mathrm{mm}$, and $R_{2b} = 8\,\mathrm{mm}$.

First, let us consider the specifics of electron beam dynamics in the proposed virpertron scheme. The longitudinal dynamics of the electrons is illustrated in Fig. 2, which shows the evolution of the beam phase-space portrait when the permittivity of the dielectric insert is $\varepsilon_1 = 5$ and when the Cherenkov radiation condition for the injected electrons is satisfied. Initially, VC is formed in the second chamber. Then, the so-called squeezed state of a beam (SSB) begins to spread from the VC in the direction opposite to the electron beam injection. The squeezed state is a distributed VC along the length of the device and constitutes a dense high-temperature electron plasma.[23] Such behavior of the electron beam is typical for traditional magnetically insulated vircators.[23–25]

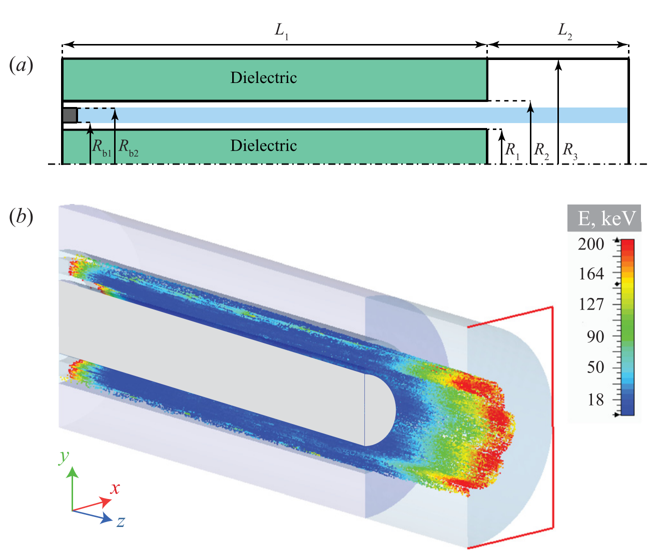

FIG. 1. (a) Virpertron design sketch plotted on the assumption of radial symmetry of the drift space. All geometrical parameters mentioned in this sketch are described in the text. (b) 3D model of the virpertron simulated in CST Particle Studio 2016. Here, charged particles are colored according to the value of their energy; $\varepsilon_1 = 4$.

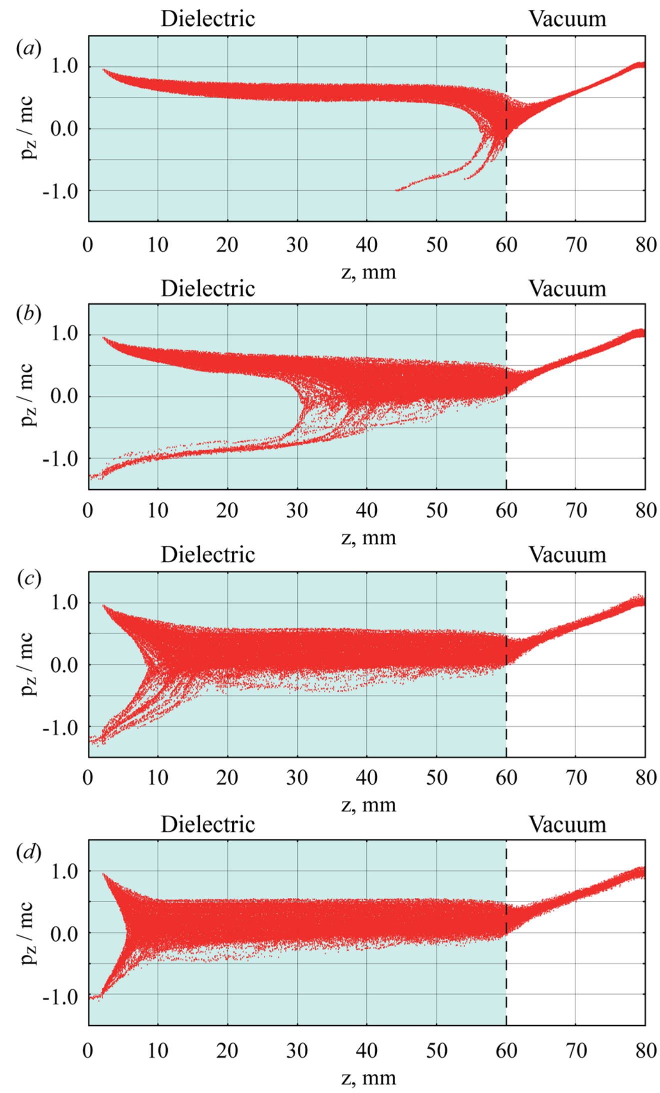

FIG. 2. Phase portraits of the electron beam in the virpertron plotted in the coordinate system "normalized longitudinal momentum p_z versus longitudinal coordinate z" in the following time moments: 1.5 ns, 2 ns, 2.5 ns, and 3 ns. Here, the relativistic momentum of the particles is normalized to mc, where m is the electron mass and c is the speed of light.

III. MICROWAVE GENERATION

Electromagnetic processes in the virpertron are different from the processes that occur in traditional magnetically insulated vircators. It is known[21] that the latter exhibit usually one characteristic frequency of microwave generation (f_{VC}) which is determined by the plasma frequency of the electron beam. Virtual cathode oscillations as a whole are responsible for this frequency. The virpertron demonstrates in the working mode a two-frequency regime of microwave generation: the lower frequency (f_{VC}) corresponds also to virtual cathode oscillations and the higher (f_{Ch})—to the Cherenkov radiation due to the fact that the mean velocity of electrons in SSB exceeds the phase velocity of the electromagnetic wave in the waveguide with a dielectric insert.

Let us consider the evolution of beam dynamics and electric field oscillation spectra (E_z-components) in the middle of the first chamber with an increasing permittivity, ε_1 (Fig. 3). These spectra reflect well the spectral distributions

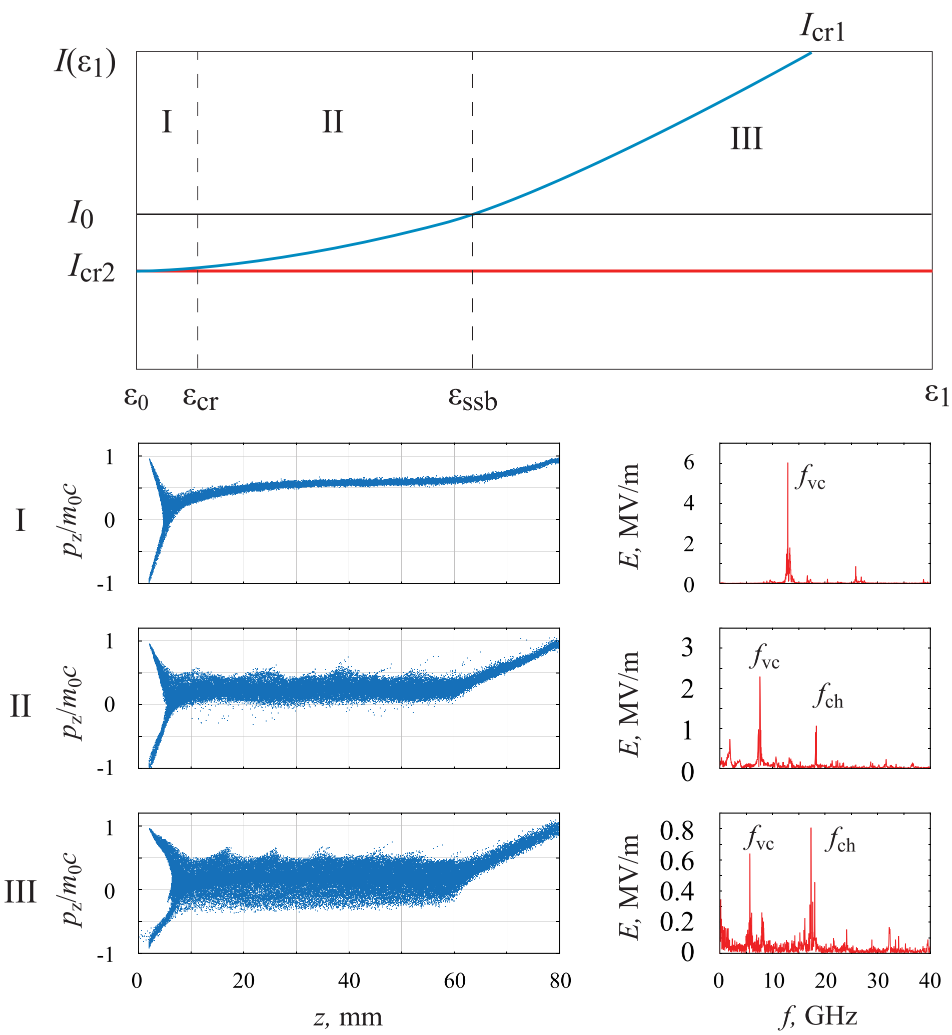

FIG. 3. (Upper panel) Qualitative dependence of the critical current I_{cr1} of the first chamber on the value ε_1 of permittivity of the dielectric insert (blue curve) with marked lines of the critical current I_{cr2} of the second chamber (red line) and beam current I_0 (dashed line); I, II, and III denote the areas with different system dynamics: I—classic mechanism of VC formation when it forms in the first chamber only; II—the regime with poorly developed SSB: VC forms initially in the first chamber, another less developed VC forms in transit after the first VC current at the junction between the first and second chambers; III—the regime with classic well-developed SSB. ε_{cr}—the value of permittivity that divides regimes I and II, and $\varepsilon_{cr} \gtrsim \varepsilon_0 = 1$; so, area I is narrow; ε_{ssb}—the value of permittivity that divides regimes II and III, which is determined by the point of intersection of the beam current line and the dependence $I_{cr1}(\varepsilon_1)$. Typical phase portraits of the electron beam in the virpertron and Fourier spectra of E_z-field oscillations obtained using the probe located in the first chamber of the virpertron in regimes I ($\varepsilon_1 = 1$), II ($\varepsilon_1 = 2$), and III ($\varepsilon_1 = 4$) are shown in the lower panel; time moment – 12 ns.

of oscillatory processes that occur in the electron beam with a virtual cathode. When value ε_1 is close to 1, the system demonstrates the "classic" mechanisms of virtual cathode formation and oscillations leading to single-frequency generation (Fig. 3, regime I); the condition for the Cherenkov radiation (electron velocities are greater than electromagnetic wave velocity) is not fulfilled in this case.

At permittivities $\varepsilon_1 > 1$, beam dynamics depends significantly on the relationship between beam current and critical space-charge limiting current of the chambers. When $\varepsilon_{cr} < \varepsilon_1 < \varepsilon_{ssb}$ (ε_{ssb} is the character permittivity value for which the beam current equals the critical current of the first chamber), the critical current of the first (and obviously the second) chamber is less than the beam current and a virtual cathode is formed initially in the first chamber. Then, less developed secondary VC forms in transit after the first VC current at the junction between the first and second chambers and SSB is established between the VCs (Fig. 3, regime II). SSB is poorly developed in this regime: the beam phase portrait demonstrates the almost complete absence of reflected electrons in the SSB region with the mean energy of electrons being essentially greater than zero. The second Cherenkov frequency component f_{Ch} appears in the spectrum in this case, and its value is determined by the intersection point of the dispersion line of the space-charge wave in the electron beam and the dispersion characteristics of the waveguide that has the form of the first chamber with the dielectric (see Fig. 4). A space-charge wave emerges in SSB due to the modulation of the passing part of the beam by the first VC

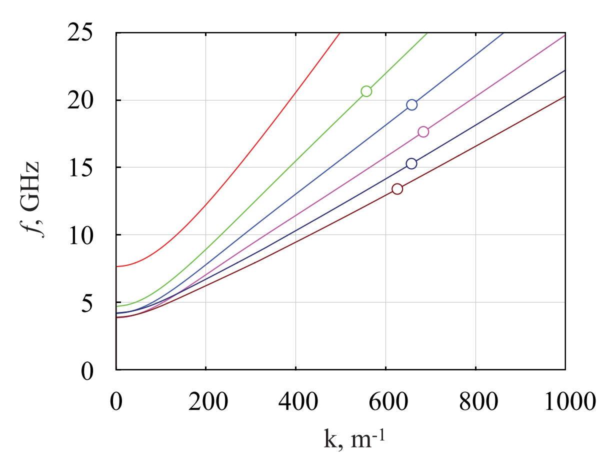

FIG. 4. Dispersion characteristics of the waveguide in the form of the first chamber with a dielectric for different values of permittivity of the dielectric insert (bottom-up): $\varepsilon_1 = 6$; 5; 4; 3; 2; 1. Circles denote the points of intersections of the waveguide dispersion characteristics with the dispersion lines of the space-charge wave in the electron beam. k is the wave number.

oscillations; the character signs of the space-charge wave can be observed in phase portraits in regimes II and III (see the upper boundary of SSB in phase portraits in Fig. 3). It should be noted that the offset and inclination of a space-charge wave dispersion line and, consequently, the coordinates of intersection points are determined by plasma frequency and mean energy of the propagating beam at the given permittivity. The analysis shows that the intersections exist for $\varepsilon_1 \geq 2$.

Finally, a well-developed "classic" SSB is established in the system, when $\varepsilon_1 > \varepsilon_{ssb}$ (see Fig. 3, regime III). Dynamics of such a process is described in Sec. II. The spectrum possesses a characteristic two-frequency form with a maximum amplitude value of frequency f_{Ch} and a low power noise background conditioned by the character beam dynamics. Actually, the electrons in a SSB possess a lower average velocity and demonstrate a wide velocity spread. This causes the more noisy character of the spectrum in the Cherenkov mode because Cherenkov resonance occurs at various frequencies for electrons that move with various velocities. Nevertheless, the physical cause for excitation of the Cherenkov frequency component with a maximal amplitude (f_{Ch}) is similar to regime II.

Figure 5 demonstrates the distribution of the longitudinal component of electric field E_z in the system at the Cherenkov frequency f_{Ch}. One can see that Cherenkov electromagnetic waves propagate in the inner and outer dielectric inserts, and the inner wave is more intense. So, exclusion of the inner rod will disrupt the condition for the Cherenkov effect development in the system. Also, Fig. 5 shows the transformation of the electromagnetic wave configuration at the junction between the chambers. It should be noted that the self-consistent electric field is nonzero inside the beam because annular geometry of the beam is distorted (it becomes azimuthally and longitudinally asymmetrical) due to the development of beam instabilities (e.g., Bursian and diocotron).[17]

One of the differences between the virpertron and the vircator is that the values of both frequencies can be tuned by varying the ε_1 value. This is illustrated in Fig. 6, which shows the dependencies of f_{VC} and f_{Ch} on ε_1. Clearly, with increasing permittivity, the frequency values decrease monotonically. The virtual cathode frequency decreases because

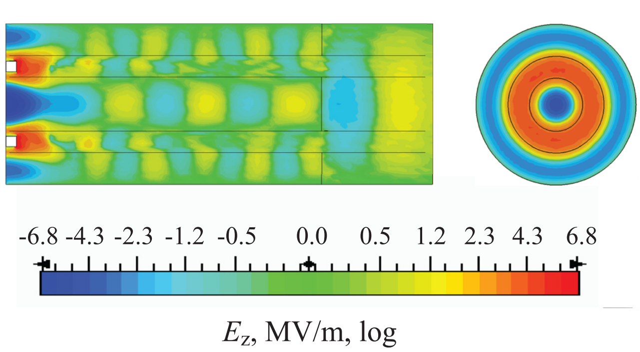

FIG. 5. Distribution of the longitudinal component of electric field E_z in the system at the Cherenkov frequency $f_{Ch} = 17$ GHz in a fixed phase. The left figure shows the longitudinal section of the system at $x = 0$ mm and right figure—cross-section at $z = 10$ mm (at the VC area); $\varepsilon_1 = 4$; time moment – 12 ns.

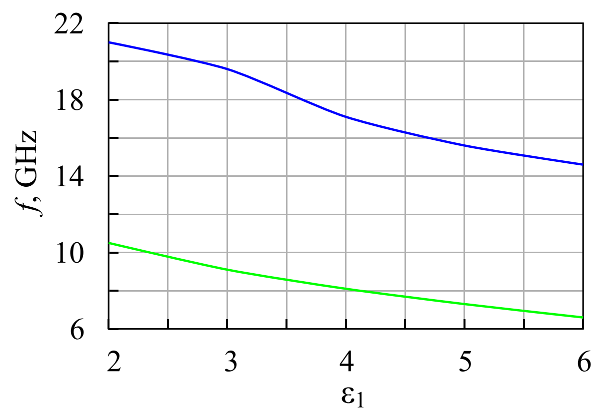

FIG. 6. Dependencies of microwave generation frequencies f_{VC} (green line) and f_{Ch} (blue line) on the permittivity of the first chamber ε_1.

the self-consistent electric field of the beam is reduced by the dielectric insert. This also explains the amplitude reduction of the components in the spectrum with the growth of ε_1. The frequency of the Cherenkov radiation is reduced as a result of the mean beam energy change and transformation of waveguide dispersion characteristics with the change in the permittivity of the insert (compare the positions of intersection points in Fig. 4 for different values of ε_1).

The mode structure of microwave oscillations in the virpertron has been analyzed. It has been discovered that two lowest order TM-modes are excited most efficiently in a waveguide output port that simulates a vacuum circular waveguide. Meanwhile, when the permittivity of the inserts in the first chamber is low ($\varepsilon_1 < 3$), the frequency f_{VC} prevails in the spectrum of the first mode and f_{Ch} prevails in the spectrum of the second one. When $\varepsilon_1 > 3$, the spectra of both modes include components with commeasurable amplitudes at frequencies f_{VC} and f_{Ch}. Of note, at high values of $\varepsilon_1 > 5$, the first mode spectrum becomes distinctly noisier.

Thus, using numerical simulations, the features of virpertron operation have been demonstrated as well as the new functionalities, which are integrated into the device concept (i.e., two-frequency generation and control over frequencies).

IV. CONCLUSIONS

We have suggested for the first time a novel scheme of a virtual cathode oscillator—virpertron—where the virtual cathode forms while the relativistic electron beam propagates through the drift space filled with dielectric materials with different values of permittivity. As we have shown, the condition $\varepsilon_1 > \varepsilon_2$ imposed on the dielectric materials leads to the implementation of the condition for limiting current $I_{lim1} > I_{lim2}$ that is necessary for the virtual cathode oscillator operation. We have obtained several important features of virpertron operation during the detailed numerical investigation of virtual cathode formation and electron-wave interaction processes in such a device. The most interesting of them is the excitation of the Cherenkov radiation in the system as the space-charge wave velocity exceeds the phase velocity of the electromagnetic wave in the chamber with the dielectric insert. We have shown the significant influence of the Cherenkov effect on the spectrum of microwave radiation in the virpertron and found out that it is responsible for excitation of the second (higher) frequency component at the output signal and for the appearance of the noise background.

We believe that the discovered effects appear to be useful for a wide range of technical applications where two-frequency high-power microwave radiation is necessary, namely, communication and radiolocation, nonlinear antennas and radars, and transition to the sub-THz frequency range. Note that it is necessary to take into account the effect of dielectric charging[26] in the practical development of the virpertron; however, this question requires further detailed investigations.

The described phenomena of the relativistic beam drift in the dielectric-filled tube may also be interesting for relevant scientific problems related to the propagation of charged particles through the waveguides composed of artificial materials, in particular, different types of metamaterials. Moreover, the obtained results have fundamental importance in terms of analysis of complex processes occurring in the new type of virtual cathode oscillator.

ACKNOWLEDGMENTS

This study was supported by the Ministry of Education and Science of the Russian Federation (Project No. 3.859.2017/4.6) and by the President's program (Project No. MK-1163.2017.2). N.S.F. acknowledges individual financial support from the Russian Foundation for Basic Research (Grant No. 16-32-60107). A.E.H. acknowledges the Ministry of Education and Science of the Russian Federation (Project No. 3.4593.2017/6.7).

[1] R. A. Mahaffey, P. A. Sprangle, J. Golden, and C. A. Kapetanakos, "High-power microwaves from a non-isochronous reflecting electron system," Phys. Rev. Lett. **39**, 843 (1977).
[2] A. N. Didenko, Y. Krasik, S. P. Perelugin, and G. P. Fomenko, "Generation of power microwave radiation of relativistic beam in triode system," Tech. Phys. Lett. **5**, 321 (1979).
[3] D. J. Sullivan, J. E. Walsh, and E. A. Coutsias, "Virtual cathode oscillator (vircator) theory," in *High Power Microwave Sources*, edited by V. L. Granatstein and I. Alexeff (Artech House Microwave Library, 1987), Vol. 13.
[4] R. F. Hoeberling and M. V. Fazio, "Advances in virtual cathode microwave sources," IEEE Trans. Electromagn. Compat. **34**, 252–258 (1992).
[5] A. E. Dubinov and V. D. Selemir, "Electronic devices with virtual cathodes (review)," J. Commun. Technol. Electron. **47**, 575 (2002).
[6] S. A. Kurkin and A. E. Hramov, "Virtual cathode formation in annular electron beam in an external magnetic field," Tech. Phys. Lett. **35**, 23–25 (2009).
[7] A. S. Shlapakovski, T. Queller, Y. P. Bliokh, and Y. E. Krasik, "Investigations of a double-gap vircator at sub-microsecond pulse durations," IEEE Trans. Plasma Sci. **40**, 1607–1617 (2012).
[8] N. S. Phrolov, A. A. Koronovskii, Y. A. Kalinin, S. A. Kurkin, and A. E. Hramov, "The effect of an external signal on output microwave power of a low-voltage vircator," Phys. Lett. A. **378**, 2423–2428 (2014).
[9] S. A. Kurkin, N. S. Frolov, A. O. Rak, A. A. Koronovskii, A. A. Kurayev, and A. E. Hramov, "High-power microwave amplifier based on overcritical relativistic electron beam without external magnetic field," Appl. Phys. Lett. **106**, 153503 (2015).
[10] J. Benford, J. A. Swegle, and E. Schamiloglu, *High Power Microwaves*, *Series in Plasma Physics*, 3rd ed. (CRC Press, Taylor and Francis Group, 2016).
[11] L. S. Bogdankevich and A. A. Rukhadze, "Stability of relativistic electron beams in a plasma and the problem of critical currents," Sov. Phys. Usp. **14**, 163 (1971).
[12] A. E. Hramov, S. A. Kurkin, A. A. Koronovskii, and A. E. Filatova, "Effect of self-magnetic fields on the nonlinear dynamics of relativistic electron beam with virtual cathode," Phys. Plasmas **19**, 112101 (2012).
[13] E. D. Poezd, A. D. Poezd, and V. Fiala, "Nonstationary processes in a Cerenkov VHF generator with dielectric loading," Czech. J. Phys. B **38**, 1005–1014 (1988).
[14] S. V. Dergunov, A. E. Dubinov, Yu. I. Kornilova, S. K. Saĭkov, V. D. Selemir, and V. P. Tarakanov, "Electron dynamics and kinetics during the formation of a virtual cathode in different media," Plasma Phys. Rep. **32**, 9–24 (2006).
[15] S. H. Gold and G. S. Nusinovich, "Review of high-power microwave source research," Rev. Sci. Instrum. **68**, 3945–3974 (1997).
[16] M. C. Balk, "Simulation possibilities of vacuum electronic devices with CST Particle Studio," in IEEE International Vacuum Electronics Conference, 2008 (IVEC-2008) (2008), pp. 459–460.
[17] S. A. Kurkin, A. A. Badarin, A. A. Koronovskii, and A. E. Hramov, "The development and interaction of instabilities in intense relativistic electron beams," Phys. Plasmas **22**, 122110 (2015).
[18] S. Champeaux, P. Gouard, R. Cousin, and J. Larour, "3-D PIC numerical investigations of a novel concept of multistage axial vircator for enhanced microwave generation," IEEE Trans. Plasma Sci. **43**, 3841–3855 (2015), ISSN 0093-3813.
[19] D. J. Sullivan, "High–power microwave generator using relativistic electron beam in waveguide drift tube," U.S. patent 4345220 (17 August 1982).
[20] D. J. Sullivan, "High power microwave generation from a virtual cathode oscillator (vircator)," IEEE Trans. Nucl. Sci. **30**, 3426–3428 (1983).
[21] R. D. Scarpetti and S. C. Burkhart, "The study of a reflex oscillator used to generate high-power microwaves," IEEE Trans. Plasma Sci. **13**, 506–512 (1985).
[22] W. Jiang, K. Masugata, and K. Yatsui, "Mechanism of microwave generation by virtual cathode oscillation," Phys. Plasmas **2**, 982–986 (1995).
[23] A. M. Ignatov and V. P. Tarakanov, "Squeezed state of high-current electron beam," Phys. Plasmas **1**, 741–744 (1994).
[24] A. E. Dubinov, "Scenario for the establishment of an electron beam squeezed state in a magnetically insulated vircator," Tech. Phys. Lett. **23**, 870–871 (1997).
[25] A. G. Petrik, S. A. Kurkin, A. A. Koronovskii, and A. E. Hramov, "3D simulation of electron beam squeezed-state generation in a two-section drift tube and analysis of its characteristics," Tech. Phys. Lett. **42**, 792–795 (2016).
[26] D. Shiffler, J. Luginsland, D. M. French, and J. Watrous, "A Cerenkov-like maser based on a metamaterial structure," IEEE Trans. Plasma Sci. **38**, 1462–1465 (2010), ISSN 0093-3813.
[27] A. E. Dubinov and I. N. Kitayev, "Child-Langmuir law for a planar diode filled with a two-layer dielectric," IEEE Trans. Plasma Sci. **44**(10), 2376–2381 (2016).